Journal of Digital Imaging

Application of QC_DR Software for Acceptance Testing and Routine Quality Control of Direct Digital Radiography Systems: Initial Experiences using the Italian Association of Physicist in Medicine Quality Control Protocol

Andrea Nitrosi,[1] Marco Bertolini,[1] Giovanni Borasi,[1] Andrea Botti,[1] Adriana Barani,[1] Stefano Rivetti,[2] and Luisa Pierotti[3]

Ideally, medical x-ray imaging systems should be designed to deliver maximum image quality at an acceptable radiation risk to the patient. Quality assurance procedures are employed to ensure that these standards are maintained. A quality control protocol for direct digital radiography (DDR) systems is described and discussed. Software to automatically process and analyze the required images was developed. In this paper, the initial results obtained on equipment of different DDR manufacturers were reported. The protocol was developed to highlight even small discrepancies in standard operating performance.

KEY WORDS: Quality control, direct digital radiography, automatic software, quality assurance, automated measurement, image quality analysis

INTRODUCTION

In recent years, radiographic systems have undergone the "digital revolution," but the quality control protocols for digital imaging equipment still remain in a quite early stage of development. In principle, the implementation of a quality assurance (QA) program for direct digital radiography (DDR) equipment could be derived from existing national and international standards.[1–6] The execution of a quality assurance protocol in a clinical environment should be rapid, and the analysis and the verification of the results should be obtained in very short time. In addition, each department could have different equipment (manufacturer, software release, etc.). These aspects require a highly flexible and automated QA protocol. The intrinsic nature of digital images produced by DDR systems allows the "online" use of automated quality control software.

METHODS AND MATERIALS

In order to establish a generally acceptable baseline performance of the systems, a total of 14 DDR systems from four manufacturers were periodically tested and their results compared in the framework of the Digital Quality Assurance Task Group of the Italian Association of Physics in Medicine (AIFM; Table 1). All the tests were done in a clinical environment.

In order to verify the temporal trend of the state of calibration, the protocol was repeated periodically on the same system (a Philips Digital Diagnost): the first evaluation just after the initial calibration and after 1, 2, 3, and 4 weeks (for this

[1]*From the Servizio di Fisica Sanitaria, Azienda Ospedaliera Santa Maria Nuova, Reggio Emilia, Italy.*

[2]*From the Servizio di Fisica Sanitaria, AUSL, Modena, Italy.*

[3]*From the Servizio di Fisica Sanitaria, AOU Sant'Orsola-Malpighi, Bologna, Italy.*

Correspondence to: Andrea Nitrosi, Servizio di Fisica Sanitaria, Azienda Ospedaliera Santa Maria Nuova, Reggio Emilia, Italy; tel: +39-0522-296076; fax: +39-0522-296392; e-mail: nitrosi.andrea@asmn.re.it

Online publication 3 September 2008

doi: 10.1007/s10278-008-9150-z

Table 1. List of DDRs Tested and Calibration Conditions

Manufacturer and product name	No. of systems	No. of controls	Calibration conditions
Philips Digital Diagnost	6	24	SID 110/150 cm; 70 kVp; 21 mm Al[a]; no grid
GE Definium	4	16	SID 180 cm; 70 kVp; 20 mm Al[a]; no grid
Siemens Axiom Aristos FX	2	8	SID 180 cm; 70 kVp; 0.5 mm Cu + 1 mm Al[a]; no grid
Kodak DR7500	2	4	SID 110/183 cm; 70 kVp; 0.5 mm Cu + 1 mm Al[a]; no grid

[a]Intended as additional x-ray tube filtration

system, the manufacturer requires a monthly calibration).

The image information acquired from a DDR system is not immediately suitable for image display. The images must be corrected in order to remove some artifacts and to correct their appearance to obtain a diagnostic radiogram.[7]

All manufacturers strongly suggest a periodic repetition of detector calibration ("flat field"). The results are influenced by the filtration, the presence of the grid, and the distance between the x-ray source and the detector. This correction is very critical and, if not carefully done, can contribute to image degradation. For this reason, the detector testing should be done under the same conditions of the calibration stage as indicated by the manufacturer.

The exposure level on the detector should be chosen in the same range as in the clinical practice. This exposure level is called the "normal level"[2] and should be specified by the manufacturer (otherwise estimated on the basis of clinical image analysis).

All the evaluations should be performed on the raw preprocessed images (digital images obtained after flat field, dark noise, and defective pixel corrections, but without any post processing filtering).

For one manufacturer (Philips), it was impossible to obtain, in clinical conditions, nonpreprocessed (unfiltered) images.

If the pixel values are not linear with respect to air kerma, they should be linearized using the proper response curve.[8]

In this study, the images were acquired under various exposure conditions using the test objects indicated below.

The data processing software[9] was developed with IDL rel. 6.4 (ITT Visual Information Solutions, Boulder, CO, USA); all the images were evaluated using this software. This software, named QC_DR, is freely available at http://www.qcdr.org.

Test Objects Used

MTF and Lag Tool

The test device for the determination of the modulation transfer function (MTF) and the magnitude of lag effects is described by the IEC 62220-1 and consists of a 1.0-mm-thick tungsten plate, 100 mm long and 75 mm wide.[2]

Low-Contrast Detectability Tool

The low-contrast Leeds phantoms and Artinis M.S. CDRAD low-contrast phantoms are used to create automated contrast–detail curves.

Tests Performed

The set of quality control procedures described are basically derived by the IEC standards and should represent an "operative" protocol translation in the clinical environment. The protocol adopted proposes additional controls (e.g., uniformity tests, defective pixel analysis, etc.) in order to check clinical relevant images quality aspects.

The complete lists of quality controls testing parameters proposed are reported in Table 2. In the second column of the table, the sections where they are more extensively described are reported, too.

Conversion Function

Purpose To establish the relationship between detector dose and pixel value in a range compatible with clinical conditions.[2]

Method A calibrated dosimeter is positioned approximately at half the source-to-detector distance using correct acquisition geometry in order to minimize the backscattered radiation from layers behind the detector. The detector surface exposure is then computed at a reference point

Table 2. List of DDR Quality Controls

Testing parameter	Section in the article
Conversion function	Conversion function
Dark image analysis	Dark image
Nonuniformity	Nonuniformity
Noise analysis	Noise
Artifacts	Defective pixels analysis
Spatial resolution	Spatial resolution
Low contrast	Low-contrast detectability
Lag	Lag

applying the inverse square law and, if necessary, detector position correction factor.

Acquire constant intensity x-ray exposure images across the full area of the detector (flat image), using at least eight different tube loadings (in milliampere second).[10] Choose the minimum possible milliampere second loading in order to obtain the kerma level on the surface of the detector corresponding to the minimum kerma level achievable, and choose the maximum milliampere second so as to avoid any saturation effects given by the detector manufacturer specifications.

Fit the mean pixel value in function of kerma by a model function (specified by the manufacturer) in order to obtain a linearized image with respect to the air kerma.

Pass/Fail Criteria Evaluate accuracy and precision of the conversion function: as stated in the IEC 62220-1 standard, the fit result has to fulfill a "final $R^2 \geq 0.99$ and no individual experimental data point deviates from its corresponding fit result by more than 2% relatively."[2]

Dark Image

Purpose To assess the intensity of intrinsic noise in the system.

Method Place a lead attenuator (of at least 2 mm thick) at the x-ray output source. Close the collimators as much as possible. Set the kilovoltage peak and milliampere second as low as possible (e.g., 40 kVp and 0.5 mAs)

Acquire a constant intensity x-ray exposure images across the full area of the detector ("dark image"). Evaluate the mean signal on the surface of the detector in five regions of interest (ROI) of at least 200×200 pixels positioned in the center of the detector and in each image sector.

The measured values should correspond to the offset (electronic noise signal) of the detector.

It is important to note the different approach adopted from the main flat panel detector (FPD) manufacturers in order to correct the image offset using the self-scanned nature of the detectors.

For example, the offset correction for the Trixell detector is typically done automatically by measuring the image response just before or after an exposure, allowing the system to correct variations in dark current with time and temperature.

Pass/Fail Criteria For each ROI, the ratio between the mean values and the normal level should not differ more than 2% in order to comply with the conversion function control limits.[2,11]

Nonuniformity

Purpose To test the flat field correction by evaluating a uniform flat image and the conversion function consistency over the full area of the detector.

Method Set milliampere second in order to have an incident kerma level on the surface of the detector near equivalent to the normal exposure level.

Acquire a full-field uniform image.

Evaluate the mean signal and its standard deviation (SD) in consecutive 3×3 cm square ROIs overlapped by 1.5 cm each, omitting the edge of the image within about 3 cm (equal to about the 2% of the source-to-image distance in collimator light-to-x-ray field total misalignment along either the length or the width of the x-ray field);[12] in addition, in good practice boundaries, areas should not have any diagnostic significance.

The effective analyzed area must be at least the 80% of the whole detector area.

Assess the nonuniformity evaluation locally (or differential) and globally for the signal and signal to noise ratio (SNR) intensity as explained below.

Local signal nonuniformity (LSNU) should be evaluated as the mean signal intensity difference between two consecutive ROIs (in each spatial direction):[11]

$$\mathrm{LSNU} = \max\left(\frac{\max\left(\left|\overline{\mathrm{ROI}}_{i,j} - \overline{\mathrm{ROI}}_{i\pm1,j\pm1}\right|\right)}{\overline{\mathrm{ROI}}_{i,j}}\right) \quad (1)$$

where $\overline{\mathrm{ROI}}_{i,j}$ is the mean value of the (i,j)-th ROI.

Global signal nonuniformity (GSNU) should be evaluated as the difference between the maximum and the minimum mean signal intensity found in all the ROIs:

$$\mathrm{GSNU} = \frac{\max\left(\overline{\mathrm{ROI}}_{i,j}\right) - \min\left(\overline{\mathrm{ROI}}_{i,j}\right)}{\left(\max\left(\overline{\mathrm{ROI}}_{i,j}\right) + \min\left(\overline{\mathrm{ROI}}_{i,j}\right)\right)/2} \quad (2)$$

where $\overline{\mathrm{ROI}}_{i,j}$ has the same definition given previously.

Similarly, the local SNR nonuniformity (LSNRNU) should be evaluated as signal to noise intensity difference between two consecutive ROIs (in each spatial direction):

$$\mathrm{LSNRNU} = \max\left(\frac{\max\left(\left|\frac{\overline{\mathrm{ROI}}_{i,j}}{\sigma\left(\mathrm{ROI}_{i,j}\right)} - \frac{\overline{\mathrm{ROI}}_{i\pm1,j\pm1}}{\sigma\left(\mathrm{ROI}_{i\pm1,j\pm1}\right)}\right|\right)}{\frac{\overline{\mathrm{ROI}}_{i,j}}{\sigma\left(\mathrm{ROI}_{i,j}\right)}}\right) \quad (3)$$

where $\overline{\mathrm{ROI}}_{i,j}$ is the mean value of the (i,j)-th ROI and $\sigma(\mathrm{ROI}_{i,j})$ is the SD of the (i,j)-th ROI.

Global SNR nonuniformity (GSNRNU) should be evaluated as the difference between the maximum and the minimum SNR intensity found in all the ROIs:

$$\mathrm{GSNRNU} = \frac{\max\left(\frac{\overline{\mathrm{ROI}}_{i,j}}{\sigma\left(\mathrm{ROI}_{i,j}\right)}\right) - \min\left(\frac{\overline{\mathrm{ROI}}_{i,j}}{\sigma\left(\mathrm{ROI}_{i,j}\right)}\right)}{\left(\max\left(\frac{\overline{\mathrm{ROI}}_{i,j}}{\sigma\left(\mathrm{ROI}_{i,j}\right)}\right) + \min\left(\frac{\overline{\mathrm{ROI}}_{i,j}}{\sigma\left(\mathrm{ROI}_{i,j}\right)}\right)\right)/2} \quad (4)$$

where $\overline{\mathrm{ROI}}_{i,j}$ and $\sigma(\mathrm{ROI}_{i,j})$ have the same definitions given previously.

Pass/Fail Criteria The reference limits for signal and SNR intensity nonuniformity evaluation are reported in Table 3.

The rationale of the proposed limits is derived by the error propagation theory. As stated in IEC 62220-1, "no individual experimental data point deviates from its corresponding fit result by more than 2% relatively," than assuming 2% the maximum percentage error in the mean value for one ROI ($\varepsilon_{\mathrm{ROI}}$), the maximum percentage error in the difference for two adjacent ROIs is two times $\varepsilon_{\mathrm{ROI}}$, i.e., 4%. Local differences maximum percentage error in the SNR is assumed to be double with respect to the simple difference in the local average difference, taking into account the error propagation theory in the ratio of mean value and SD (approximately 4 $\varepsilon_{\mathrm{ROI}}$).

Table 3. Reference Limits Proposed for Nonuniformity Tests

Test	Reference limit (%)
Local signal nonuniformity	<4
Global signal nonuniformity	<8
Local SNR nonuniformity	<8
Global SNR nonuniformity	<20

Analogously, the global maximum percentage signal and SNR nonuniformity errors were assessed to be 8% and 20%, respectively.

Noise

Purpose To evaluate the system noise in terms of both electronic and spatial characteristics.

Method Noise power spectrum (NPS): NPS has the advantage of characterizing the spatial frequency content of image noise. The method for its calculation is explained in the IEC 62220-1 standard.[2]

Relative standard deviation (RSD) analysis: The trend of the RSD versus the exposure can give a useful insight into noise properties. For this purpose, all the images should be converted into dose acquired for the conversion function test.[10,11] The RSD, which is the ratio between the SD and the average signal value in a ROI of at least 400× 400 pixels positioned in the center of the images, should be measured.

The trend of the mean square RSD versus the exposure level should be fitted using the following function:

$$\mathrm{RSD}^2 = \left(\frac{\sigma_{\mathrm{TOT}}}{x}\right)^2 = \frac{\alpha}{x} + \beta + \frac{\gamma}{x^2} \quad (5)$$

where x is the x-ray exposure, α represents the contribution of the quantum statistical noise, β is the multiplicative contribute to noise related to a fixed-pattern noise unresolved by flat field correction, and γ is the additive factor that can be interpreted as the noise connected to electronics.[13]

Pass/Fail Criteria NPS There are no established criteria or limits for this test that should be

performed in the commissioning/acceptance test, but it could be useful in order to evaluate any grid suppression tool on the images if the calibration of the detector has to be performed with the grid inserted. If the calibration of the detector has to be performed with the grid, the presence of discrete spikes at spatial frequencies corresponding to the interline spacing of the grid should indicate an imperfect grid suppression. Presence of discrete spikes in NPS should not be observed with respect to the acceptance test, also if blotches or small single-point artifacts do not have enough power to demonstrate a measurable change in the NPS.[14]

RSD As for NPS, we do not propose any criteria or limits. α, β, and γ values should be registered and compared with the reference value fixed in the acceptance testing control. This test should give information about the DDR electronics functionality and about flat field correction effectiveness.

Defective Pixels Analysis

Purpose To check the accuracy of the defective pixels/lines correction in the preprocessing stage.[15] Ask the manufacturer for a "defective pixel map," which specifies the dead pixels location, individual pixels, pixel clusters, and lines of contiguous pixels that fail to produce a useable output value.[16] In early flat panel plates, defective pixels may represent about 0.3% of the total number of pixels. Improvements in panel manufacturing procedures are steadily reducing this number.

Defective pixels are acceptable if they are not noticeable on the image, which usually occurs only if there are large clusters of defective pixels or they occur in multiple adjacent rows or columns. Manufacturers have specifications for how many defective pixels are acceptable and on how they are eventually clustered and, for this reason, noncorrectable. If the defective pixel map is not accessible, different ways to evaluate this are possible.[7]

Method Acquire a flat, full-area image at a dose near equivalent to the normal exposure level (e.g., 2.5 μGy on the detector); for this purpose, the image used before the nonuniformity test can be utilized. Divide the image into 1×1 cm ROIs.

A defective detector element ("defective pixel") is an element of the ROI where the absolute value deviates more than 20% from the mean pixel value of the ROI elements.[10] Count the total number of defective detector elements (defective pixels).

Pass/Fail Criteria After detector calibration, in normal conditions, no defective detector element shall be counted.

Spatial Resolution

Purpose To measure the detector presampling MTF in order to ensure that the hardware is performing properly and is not degrading the resolution of the image below original equipment performance levels. This test is important for systems with moving parts in the image chain (i.e., computed radiography or scanning systems);[14] so in static DDRs systems, it could be assessed only at the commissioning stage.

Method Follow the IEC 62220-1 requirements.[2]

Pass/Fail Criteria The IEC 62220-1 standard does not propose acceptability limits. The presampling MTF should not be different from the minimum reference values supplied from the manufacturer, taking into account experimental error propagation.

Low-Contrast Detectability

Purpose To assess and control the ability of the system to demonstrate low-contrast object.

Method Place the phantom (N.A. CDRAD or Leeds phantoms) on the detector. Follow the instructions provided by the phantom manufacturer.

In the commissioning test, acquire at least six images moving the phantom slightly before each exposure (to obtain images with different relative position of the details on the detector elements) at appropriate milliampere second to deliver a dose nearly equivalent to the normal exposure level (e.g., 2.5 μGy). Repeat acquisitions following the same conditions described before changing milliampere second in order to deliver about one fourth of the normal exposure level and four times the normal exposure level (e.g., 0.6 and 10 μGy on the detector).[2,17] In routine quality control test, acquire one image at the normal exposure level.

Table 4. Constancy DDR Quality Controls and Relative Frequency

Test performed	Frequency
Conversion function	Biannual
Dark image analysis	Biannual
Nonuniformity	Biannual
Noise components	Annual
Artifacts	Biannual
Low contrast	Biannual
Lag	Biannual

Signal difference to noise (SDNR) is defined by:

$$\mathrm{SDNR} = \frac{\left|\overline{\mathrm{ROI}}_{\mathrm{signal}} - \overline{\mathrm{ROI}}_{\mathrm{background}}\right|}{\sqrt{\sigma^2_{\mathrm{signal}} + \sigma^2_{\mathrm{background}}}} \quad (6)$$

where $\overline{\mathrm{ROI}}_{\mathrm{signal}}$ and $\overline{\mathrm{ROI}}_{\mathrm{background}}$ are the mean values of the ROI within the target and of the background region near the target, respectively, and $\sigma^2_{\mathrm{signal}}$ and $\sigma^2_{\mathrm{background}}$ are the variances of the ROI within the target and of the background area near the target, respectively. Measure the SDNR for each target group.

Pass/Fail Criteria There are no established criteria or limits for this test that should be performed in the commissioning/acceptance test. This test represents a baseline for future measurements and it could allow an objective assessment of system performance by comparison of current and historical data.

In the following routine quality control tests (after detector calibration), no statistically significant difference should be measured from the baseline acceptance test.

Lag

Purpose To evaluate the severity of any artifact due to previous exposure to the detector. This effect derived from:

- a delay in generated signal being read that can cause some of the signal generated in a prior image to appear superimposed on the signal generated during the current image acquisition (additive lag);
- a temporary change in the sensitivity of the detector determined by prior exposure history (multiplicative lag).

Method Follow the IEC 62220-1 Annex A: "Determination of lag effects." Two tests are proposed: additive and multiplicative lag effects test.

Pass/Fail Criteria As stated by the IEC 62220-1 standard,[2] the lag effects must contribute less than 0.5% of the effective exposure. In Table 4, the tests and the frequency of constancy quality controls are listed.[10]

QC_DR Software

QC_DR software, following the procedures stated before, can automatically perform the image analysis necessary to obtain the conversion function and to evaluate the RSD, the dark image, the signal and SNR nonuniformity, the defective pixels, and the lag effects. The analysis is performed based on DICOM or more generally raw images (in this latter case, the user must fill the fields needed to open/elaborate the image(s), e.g., image type, width and

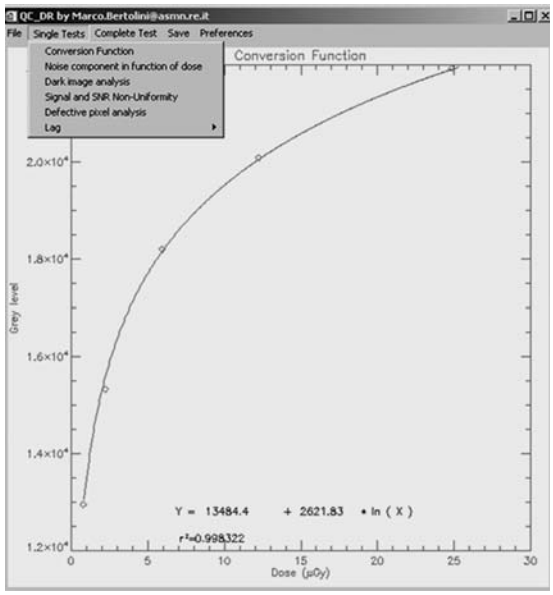

Fig 1. Depiction of the QC_DR software graphical user interface.

Table 5. Results of Constancy Quality Control Tests (The Error Corresponds to ±1 SD)

	Conversion function		Dark image analysis	Nonuniformity				Artifacts	Lag	
Test performed	R^2	Max data point deviation (%)	Mean signal (%)	LSNU (%)	GSNUS (%)	LSNRNU (%)	GSNRNU (%)	No. of defective pixel(s)	Additive	Multiplicative
Results	0.999 ± 0.001	1.69	0.9 ± 0.6	0.7 ± 0.2	3.6 ± 2	4.6 ± 1	15.5 ± 2	0	0.05 ± 0.04	0.13 ± 0.08
Reference limit proposed	>0.99	<2	<2	<4	<8	<8	<20	0	<0.5	<0.5

Table 6. Weekly Tested System Test Results (the Error Corresponds to ±1 SD)

	Conversion function		Dark image analysis	Nonuniformity				Artifacts	Noise components			Lag	
Test performed	R^2	Max data point deviation (%)	Mean signal (%)	LSNU (%)	GSNUS (%)	LSNRNU (%)	GSNRNU (%)	No. of defective pixel(s)	Quantum statistical noise (α)	Multiplicative contribute (β)	Additive factor (γ)	Additive	Multiplicative
After calibration	0.9999	0.09	0.9 ± 0.3	0.26	0.74	4.21	12.07	0	2.5E-06	9.4E-05	8.6E-04	0.02	0.05
After 1 week	0.9999	0.19	0.9 ± 0.3	0.93	1.49	4.41	12.01	0	2.6E-06	9.5E-05	8.5E-04	0.04	0.14
After 2 weeks	0.9998	0.45	1.2 ± 0.3	0.36	1.43	4.95	13.72	0	2.5E-06	9.1E-05	8.6E-04	0.06	0.27
After 3 weeks	0.9999	0.32	1.4 ± 0.3	0.32	1.46	4.4	13.71	0	2.6E-06	9.8E-05	8.9E-04	0.07	0.30
After 4 weeks	0.9999	0.30	1.1 ± 0.3	0.44	1.27	4.05	14.08	0	2.7E-06	1.0E-04	9.1E-04	0.06	0.25
Reference limit	>0.99	<2	<2	<4	<8	<8	<20	0	–	–	–	<0.5	<0.5

Table 7. Test Results of the System Before and After Calibration

	Conversion function		Dark image analysis	Nonuniformity				Artifacts	Noise components			Lag	
Test performed	R^2	Max data point deviation (%)	Mean signal (%)	LSNU (%)	GSNUS (%)	LSNRNU (%)	GSNRNU (%)	No. of defective pixel(s)	Quantum statistical noise (α)	Multiplicative contribute (β)	Additive factor (γ)	Additive	Multiplicative
Not calibrated[a]	0.9965	*14.74*	*5.32*	0.56	2.56	3.22	10.24	*54*	2.9E-05	4.3E-04	1.4E-03	0.035	0.11
After calibration	0.9999	1.7	0.12	0.77	2.05	5.90	12.49	0	8.7E-06	1.3E-04	4.8E-04	0.034	0.12
Reference limit	>0.99	<2	<2	<4	<8	<8	<20	0	–	–	–	<0.5	<0.5

Values in italics are out of limits

[a]About 90 days after last calibration

height, offset, little or big endian, pixel size, and so on). An output file can be saved in a text file (common separated value format) for further analysis or test documentation. A simplified user guide is disposable on the website.[9] In Fig. 1, a depiction of the graphical user interface (GUI) of the QC_DR software is presented.

RESULTS AND DISCUSSION

All the MTF, NPS, and detective quantum efficiency measured in the acceptance test of the checked systems conform to the manufacturer's specification and were in good agreement with the results published in the literature.[8,18–24] The results of quality control constancy tests on all systems, considering the reference values and tolerances proposed, are listed in Table 5.

The proposed baseline performance limits for constancy quality control tests on calibrated units are derived from the IEC standard and are satisfied for all the systems tested. Only the conversion function limits on the maximum data point deviation were close to the limit proposed, in particular those referred to low-dose mean pixel value signals. This was probably also due to the intrinsic dosimeter sensitivity.

The proposed baseline performance could represent the acceptable limit levels for all DDR systems. Achievable level limits, lower than the baseline ones, should be adopted for each own system on the basis of acceptance and routinely quality controls results.

As we mentioned before, on a Philips Digital Diagnost system for which the manufacturer specifications require at least a monthly flat fielding correction, the tests were repeated also 1, 2, 3, and 4 weeks after the calibration. In Table 6, the data referred to this system (called "weekly tested system") for which the tests were repeated are reported.

When visiting the center which was operating a Siemens Axiom Aristos FX system, we found that the technicians did not execute for quite a long time (about 90 days) the routine (monthly) required calibration procedure.

As could be foreseen, the system was found severely miscalibrated. After a first set of evaluation, the system was properly calibrated. In Table 7, the data referred to this system before and after the proper calibration procedure are reported.

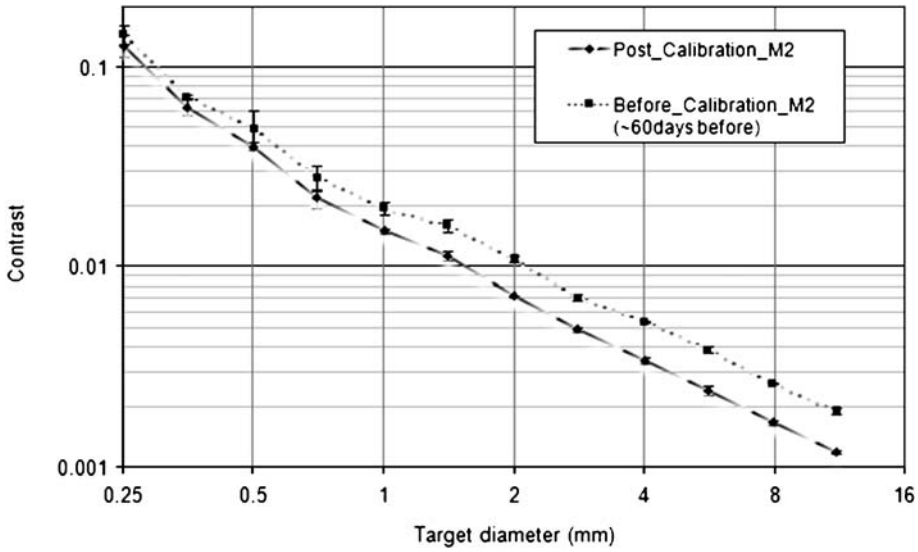

Fig 2. Contrast–detail curves obtained, taking into account two systems from the same manufacturer (error bars are referred to standard error).

For a complete constancy quality test, the time required was about 15 min per DDR system and the utilization of the automated software allowed the complete analysis of the images in less than 10 min.

Conversion Function

All DDR systems widely pass the reference limits proposed both in terms of the Pearson correlation coefficient (R^2) and of the maximum percentage experimental data point deviation. For

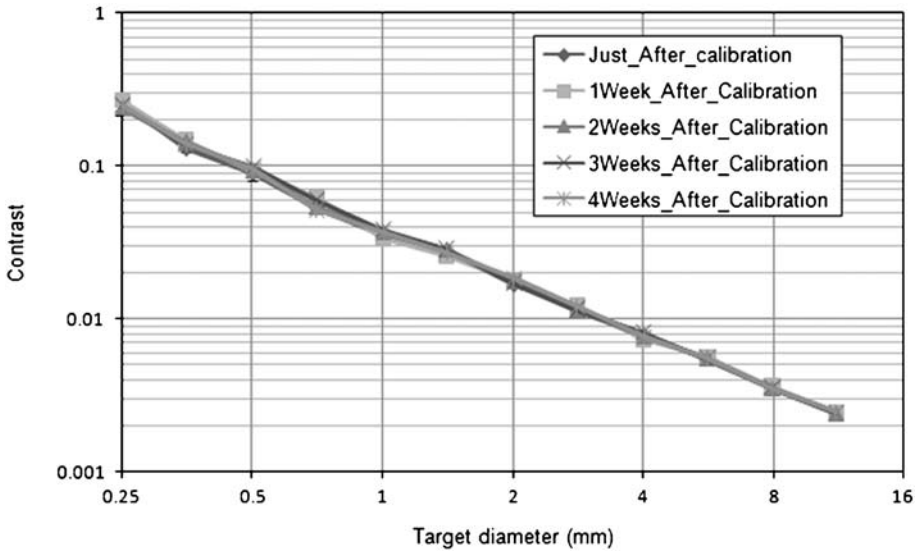

Fig 3. Contrast–detail curves measured for the same system just after calibration and repeated each week before the following manufactured requested calibration procedure.

the weekly tested system, no significant difference (considering the experimental data acquisition error propagation) was found.

The uncalibrated system passed the reference limit proposed for the correlation coefficient, but the maximum percentage experimental data point deviation was out of the limit. The limit was not met for low doses. That should be expected on the basis of the dark noise test results reported in the following paragraph.

Dark Image

Considering the experimental data acquisition error propagation, no significant difference was found in any systems after calibration. The dark image analysis did not reveal appreciable differences among tests performed 1, 2, 3, and 4 weeks after the flat fielding correction, probably due to the correct calibration timing.

For the uncalibrated system, dark image analysis revealed a significant difference on the mean signal that resulted in more than twice the limit proposed. That result is probably due to an ineffective automatic dark noise correction.

Nonuniformity

Considering the experimental data acquisition error propagation, no significant difference was found in any systems after the calibration. Similar results were found for the weekly tested system and for the uncalibrated one.

Noise

Relative Standard Deviation

Considering the experimental data acquisition error propagation, no significant difference was found in any systems after calibration and for the system for which the controls were repeated 1, 2, 3, and 4 weeks after the flat fielding correction. For the uncalibrated system, significant differences were found for the noise components with an increase of about a factor of three for each of the components.

Artifacts Analysis

After detector calibration and in weekly tests, no defective detector elements were detected, while for the uncalibrated system, there were 54 elements. All these defective pixels were corrected subsequently to the detector calibration.

Low-Contrast Detectability

The test proposed seems to have a good sensitivity in order to assess detectability degradation. Also, the calibration frequency proposed in clinical use by the manufacturer seems to be able to avoid operating outside any limits.

In Fig. 2, we report the contrast–detail curves[25,26] obtained, taking into account two systems from the same manufacturer, one of which was uncalibrated. For the first (uncalibrated) system, the curves are referred to as the precalibration and postcalibration conditions; for the second one, the results are obtained just after calibration.

Performing a two-way analysis of variance test with a 5% confidence level, it was possible to demonstrate that the difference between two calibrated systems is not statistically significant ($F(1,48)=0.11$, $p=0.74$). The curves are statistically different ($F(1,48)=15.84$, $p=0.0002$) between precalibration and postcalibration conditions.

In Fig. 2, it is worth noting that the calibration seems to improve the detection of large diameter target rather than small target detection that is principally limited by system's high-frequency MTF.[27] The contrast–detail curves of the weekly tested system are reported in Fig. 3. Differences between the curves are not statistically significant.

Lag

For all the systems checked after calibration, additive and multiplicative lag effects were in agreement with respect to the limit proposed by the IEC 62220-1 requirement. The results for the weekly tested system were in agreement with the limit proposed, but there is observed a weak increasing trend with time after the calibration.

CONCLUSIONS

Quality control tests are of fundamental importance for keeping the systems properly operating. The proposed quality control tests for DDR are quite complex and require an automated software for image analysis. When the systems were calibrated, all the tests passed within the reference

limits. The uncalibrated system was widely outside these limits. We believe that a larger imaging trial should be useful to refine the performance limits. The proposed protocol should provide an initial framework for definition of a standardized quality control program for DDRs.

ACKNOWLEDGMENTS

The authors gratefully acknowledge the collaboration of the Italian Association of Physics in Medicine (AIFM), especially Dr. Giacomo Belli, chief of the AIFM Digital Radiography Workgroup. In addition, the authors would like to express their gratitude to Dr. Andy Smith and Dr. John Yorkston for their interest in this work.

REFERENCES

1. Schreiner-Karoussou A: Review of image quality standards to control digital x-ray systems. Radiat Prot Dosim 117:23–25, 2006

2. International Electrotechnical Commission. Medical electrical equipment: characteristics of digital x-ray imaging devices—part 1: determination of the detective quantum efficiency. Document no. 62220-1. Geneva, Switzerland: International Electrotechnical Commission, 2003

3. The Kings Centre for the Assessment of Radiological Equipment: Protocols for QA of DDR System, website: http://www.kcare.co.uk/content.php?page=protocols.htm&folder=Education

4. Faulkner K: The DIMOND project and its impact on radiation protection. Radiat Prot Dosim 3–6, 2005

5. Shepard SJ et al.: Quality Control in Diagnostic Radiology. AAPM Report 74, 2002

6. Seibert JA: Acceptance Testing and Quality Control of Photostimulable Storage Phosphor Imaging Systems. AAPM Report 93, 2006

7. Beutel J, Kundel HL, Van Metter RL: Handbook of Medical Imaging—Volume 1. Physics and Psychophysics, Washington: SPIE, 2000

8. Samei E, Dobbins JT, Lo JY, Tornai MT: A framework for optimising the radiographic technique in digital x-ray imaging. Radiat Prot Dosim 114:220–229, 2005

9. Bertolini M. QC_DR program. (http://www.qcdr.org)

10. Perry N, Broeders M, de Wolf C, Törnberg S, Holland R, von Karsa L, Puthaar E: European Guidelines for Quality Assurance in Breast Cancer Screening and Diagnosis, 4th edition. Luxembourg: Office for Official Publications of the European Communities, 2006

11. Italian Association in Medical Physics (AIFM): Digital Radiology Working Group. (http://www.fisicamedica.org)

12. International Electrotechnical Commission. Medical electrical equipment: General Requirements for Safety—3. Collateral Standard: General Requirements for Radiation Protection in Diagnostic X-ray Equipment. Document no. 60601-1-3. Geneva, Switzerland: International Electrotechnical Commission, 1994

13. Monnin P, Gutierrez D, Bulling S, Lepori D, Valley JF, Verdun FR: Performance comparison of an active matrix flat panel imager, computed radiography system, and a screen-film system at four standard radiation qualities. Med Phys 32:343–350, 2005

14. Yaffe MJ, Bloomquist AK, Mawdsley GE, Pisano E, Hendrick RE, Fajardo LL, Boone JM, Kanal K, Mahesh M, Fleischman RC, Och J, Williams MB, Beideck DJ, Maidment ADA: Quality control for digital mammography: part II recommendations from the ACRIN DMIST trial. Med Phys 33:737–752, 2006

15. Floyd CE Jr, Warp RJ, Dobbins JT 3rd, Chotas HG, Baydush AH, Vargas-Voracek R, Ravin CE: Imaging characteristics of an amorphous silicon flat-panel detector for digital chest radiography. Radiology 218:683–688, 2001

16. Padgett R, Kotre CJ: Assessment of the effects of pixel loss on image quality in direct digital radiography. Phys Med Biol 49:977–986, 2004

17. Charnock P, Connolly PA, Hughes D, Moores BM: Evaluation and testing of computed radiography systems. Radiat Prot Dosim 114:201–207, 2005

18. Samei E, Flynn MJ, Chotas HG, Dobbins III, JT: DQE of direct and indirect digital radiographic system. Proc SPIE 4320:189–197, 2001

19. Samei E, Flynn MJ: An experimental comparison of detector performance for direct and indirect digital radiography systems. Med Phys 30:608–622, 2003

20. Borasi G, Nitrosi A, Ferrari P, Tassoni D: On site evaluation of three flat panel detectors for digital radiography. Med Phys 30:1719–1731, 2003

21. Granfors PR, Aufrichtig R: Performance of a 41×41 cm^2 amorphous silicon flat panel detector for radiographic imaging applications. Med Phys 27:1324–1331, 2000

22. Illers H, Buhr E, Bergmann D, Hoeschen C: Measurement of the detective quantum efficiency (DQE) of digital x-ray imaging devices according to the standard IEC 62220-1. Proc SPIE 5368:17787, 2003

23. Borasi G, Samei E, Bertolini M, Nitrosi A, Tassoni D: Contrast–detail analysis of three flat panel detectors for digital radiography. Med Phys 33:1707–1719, 2006

24. Neitzel U, Günther-Kohfahl S, Borasi G, Samei E: Determination of the detective quantum efficiency of a digital x-ray detector: comparison of three evaluations using a common image data set. Med Phys 31:2205–2211, 2004

25. Young KC, Cook JJH, Oduko JM, Bosmans H: Comparison of software and human observers in reading images of the CDMAM test object to assess digital mammography systems. Proc SPIE 7:614206.1–614206.13, 2006

26. Marshall NW: A comparison between objective and subjective image quality measurements for a full field digital mammography system. Phys Med Biol 51:2441–2463, 2006

27. Moy JP: Signal-to-noise ratio and spatial resolution in x-ray electronic imagers: is the MTF a relevant parameter? Med Phys 27:86–93, 2000